RECLAMATION

Managing Water in the West

Technical Report No. SRH-2014-26

A Deterministic Spatially-Distributed Ecohydraulic Model for Improved Riverine System Management

Final Report, Science & Technology Proposal ID 1368

U.S. Department of the Interior
Bureau of Reclamation

April 2014

Mission Statements

The mission of the Department of the Interior is to protect and provide access to our Nation's natural and cultural heritage and honor our trust responsibilities to Indian Tribes and our commitments to island communities.

The mission of the Bureau of Reclamation is to manage, develop, and protect water and related resources in an environmentally and economically sound manner in the interest of the American public.

BUREAU OF RECLAMATION
Technical Service Center, Denver, Colorado
Sedimentation and River Hydraulics Group, 86-68240

Technical Report No. SRH-2014-26

A Deterministic Spatially-Distributed Ecohydraulic Model for Improved Riverine System Management

Final Report, Science & Technology Proposal ID 1368

Prepared: Daniel Dombroski, Ph.D., P.E.
Hydraulic Engineer, Sedimentation and River Hydraulics Group 86-68240

Peer Review: Blair Greimann, Ph.D., P.E. Date
Hydraulic Engineer, Sedimentation and River Hydraulics Group 86-68240

Executive Summary

The survival of riparian vegetation within managed river systems is a growing challenge due to the increasing priority of maintaining or restoring ecosystem function while balancing the need for water supply and flood protection. Establishment, growth, and decay of riparian vegetation is largely determined by local hydraulics; conversely, characteristics of in-channel and floodplain vegetation effect hydraulics at the reach scale. Despite a wealth of prior research concerning the mechanics and biology of flow-vegetation interactions, the need for operation-level tools for making quantitative predictions remains.

The development of a coupled two-dimensional vegetation and hydraulic model developed at the Bureau of Reclamation is described. The model is based upon the SRH-2D computational software package, which contains a two-dimensional flow and mobile bed sediment transport model. The new SRH-2DV package incorporates (1) a module that simulates spatially distributed establishment, growth, and mortality of riparian vegetation and (2) a module that simulates the effect of vegetation on river and floodplain hydraulics through spatially distributed roughness. Simulation results are presented from application to simple case studies, and the utility of expanding the predictive capabilities for application to more complex systems is discussed. Results from SRH-2DV will aid the science, economics, and policy of establishing environmental flows by addressing questions regarding the physical and biological interaction of flow and vegetation in rivers and floodplains.

Contents

Page

Introduction

The survival of riparian vegetation within managed river systems is a growing challenge due to the increasing priority of maintaining or restoring ecosystem function while balancing the need for water supply and flood protection. Establishment, growth, and decay of riparian vegetation is affected by local hydraulics; conversely, characteristics of in-channel and floodplain vegetation affect hydraulics at the reach scale.

Vegetation resists flow due to drag forces on discrete elements and nonlinear interactions between multiple elements (Nepf, 2012). Flow resistance in natural systems is often characterized through the estimation of a dimensionless (e.g., Darcy friction factor *f*) or dimensional (e.g., Chezy coefficient *C* and Manning's *n*) roughness parameter that is used to model the hydraulics. Roughness parameters derive from a combination of empiricism and hydrodynamic theory and are generally interrelated deterministically. The roughness of a vegetated channel is generally a function of both the characteristics of the vegetation (e.g., size, density, flexibility, leaf area) and the flow itself (due to streamlining effects). Chow (1959) produced a list of bracketed roughness values corresponding to various vegetated flow types. Thompson & Roberson (1976) presented an analytical method for predicting roughness due to a flow through vegetation modeled as rigid or flexible cylinders. The method depends on estimation of a drag coefficient, stem spacing and diameter, and flexural rigidity. Kouwen & Li (1980) developed an iterative approach for calculating roughness as a function of vegetation rigidity, and estimated plant deflection in response to forcing exerted by the flow. The Kouwen & Li (1980) approach is generally applicable to grasses, and the authors provided a table with stiffness values for a large variety of grass types. Kouwen & Fathi-Moghadam (2000) describe methodology to estimate resistance due to coniferous trees in open-channel flow by modifying a previously existing model (Fathi-Moghadam & Kouwen, 1997) in order to account for variations in the flexibility between species. The authors obtained species-specific parameters for the equations by conducting intricate laboratory and field experiments to measure drag force on model trees. Darby (1999) presents a simplified cross-section based model for predicting roughness associated with sediment or vegetation. The approach applies one of six different empirically calibrated flow resistance equations at each computational node. An equation similar to the Kouwen & Li (1980) approach is used for flexible vegetation, while an equation similar to the Thompson & Roberson (1976) approach is used for nonflexible vegetation. A procedure for estimating roughness due to flow through stiff or flexible woody vegetation is described by Jarvela (2004). The method, limited to emergent vegetation, incorporates leaf area index (LAI) to account for the effect of leaf distribution on drag resistance. The author also presents (Jarvela, 2005) an analysis of flow structure over submerged flexible vegetation with a focus on

velocity profiles and turbulence characteristics. Baptist et al. (2007) derive a Chezy-type formulation for calculating resistance due to submerged or emergent vegetation. The representative resistance coefficient includes contributions from the bed roughness, form drag from flow through the vegetation, and shear due the velocity profile above the vegetation. Hession and Curran (2013) provide a literature review of trends and research in the topic of vegetation-induced roughness in fluvial systems; the authors discuss the spatio-temporal complexity of processes related to vegetation-flow-sediment interactions. Abu-Aly et al. (2014) present the results of two-dimensional hydraulic modeling using roughness derived from LiDAR. The authors demonstrate the effects of spatially-distributed roughness on hydraulics at the local and reach scale, and underscore the importance of systematically defining roughness at the resolution of the computational grid. The challenge of capturing the complexity of effects due to flow through a broad range of vegetation types is reflected by the diversity of predictive tools developed during more than five decades of research.

The local hydraulics within a river system in part determines the establishment, growth, and removal of riparian vegetation. Complicating the interplay between ecology and hydraulics are processes related to hydrology and climate, substrate and groundwater, and species-species interactions. The timescales of ecohydraulic processes range from short (e.g., seed dispersal, scour) to long (e.g., establishment and seasonal growth). The desire to better manage riparian vegetation has led to a body of research aimed at modeling ecohydraulic processes. Mahoney & Rood (1998) describe an integrative conceptual model that defines the hydrologic and environmental conditions required for successful Cottonwood recruitment. The authors make quantitative recommendations regarding water table and pore water recedence rates. A review of Cottonwood ecophysiology is given by Rood et al. (2003), in which physiological and morphological changes are documented due to dewatering processes within river channels. A river seeding concept (Meier, 2008) argues the importance of seed dispersal as a function of flood stage and drawdown rate, challenging aspects of the work of Mahooney & Rood (1998). Merritt & Wohl (2002) discuss vegetation recruitment and hydrochory dependencies on hydraulics, hydrology, and dispersal phenology, and suggest physical parameters relevant to a model framework. Groves et al. (2009) developed a stochastic seed dispersal model using an analytical expression with inputs dependent on local kinematics. The aforementioned studies have contributed to a better mechanistic understanding of specific ecohydraulic processes.

While many studies have advanced the understanding of focused processes related to vegetation-flow interactions, comparatively few have attempted a comprehensive modeling effort. Lytle & Merritt (2004) describe an approach to model how cycles of flood and drought affect long-term Cottonwood forest population dynamics. The stochastic matrix model predicts succession by adjusting probabilities according to environmental conditions. Hooke et al. (2005) developed a rule-based model for morphology, vegetation, and sediment changes in ephemeral streams. Perona et al. (2009) provide a review of vegetation and flow modeling using deterministic and stochastic approaches with

varying levels of simplification, and include a discussion of dynamics at relevant scales of interest. A comprehensive modeling effort by Shafroth et al. (2010) links flow events, geomorphic processes, and biotic responses. The authors used existing modeling tools (HEC-RAS, MDSWMS, MODFLOW, HEC-EFM) to simulate the effects of experimental controlled dam releases, including river morphology changes, incipient motion and scour thresholds, and stochastic vegetation response. Despite a broad base of prior work concerning vegetation-flow interactions, the need remains for a generally applicable modeling framework that can be used in a predictive sense at the operation level.

Described herein is a deterministic computational tool for modeling spatially-distributed flow and vegetation interactions. An existing two-dimensional hydraulic and sediment transport model (SRH-2D) and an existing one-dimensional hydraulic, sediment, and vegetation model (SRH-1DV), both developed at the Bureau of Reclamation (Reclamation) Technical Service Center (TSC), are used as a basis for the new model development (SRH-2DV). The SRH-2DV package includes independent modules for predicting (A) dynamic hydraulic roughness due to vegetated flow and (B) riparian vegetation lifecycle as a function of local hydraulics. The algorithms and parameters applied in the modules are drawn from a combination of published literature and collaborative research. Results from SRH-2DV will aid the science, economics, and policy regarding riparian ecosystems by addressing questions such as: (1) What impact does riparian vegetation have on local flood conditions? (2) How can vegetation be incorporated into restoration projects without increasing flood risks? (3) What set of reservoir operations can be used to encourage recruitment and survival of native vegetation (and control the spread of invasive species)? (4) How will management actions impact habitat for endangered and threatened species?

Methods

SRH-2DV Model Overview

The existing SRH-2D flow solver (Lai, Two-Dimensional Depth-Averaged Flow Modeling with an Unstructured Hybrid Mesh, 2010) is used as the computational base for the new SRH-2DV coupled flow and vegetation model. Hydraulic variables are computed by solving the depth-averaged dynamic wave equations using a finite volume numerical method. Solutions can be computed over an unstructured hybrid mesh (Lai, 1997; 2000), and the solver includes a seamless wetting-drying algorithm that is applied at each time step. With appropriate boundary conditions, constant or varying discharge flows may be simulated. The solver can compute subcritical and supercritical flow conditions without special treatment.

The SRH-2DV package features the addition of two vegetation modules: (1) The hydraulic roughness module for computing spatially-distributed Manning's *n* values based on vegetation characteristics and (2) the vegetation lifecycle module for tracking seed dispersal and plant establishment, growth, and mortality. The vegetation modules in the SRH-2DV package are coupled to the hydraulic solver; however, the modules are not presently coupled to each other. The vegetation modules receive spatially-distributed input data via a user-generated ArcGIS shapefile that is automatically mapped to the computational grid of the hydraulic solver at runtime. The computational time step for the hydraulic solver is generally limited by numerical instability, whereas the computational time step for the vegetation modules is limited by ecologically-relevant scales, and can generally be significantly larger. A larger vegetation time step offers the benefit of decreased computational overhead.

Hydraulic Roughness Module

The hydraulic roughness module computes spatially-distributed Manning's *n* values based on vegetation characteristics and hydraulic variables. Vegetation polygons are spatially delineated via an ArcGIS shapefile, where each polygon is assigned a method of computation and corresponding vegetation parameters The Jarvela (2004) and Baptist (2007) computational methods were tested. For polygons covering areas in which vegetation-based roughness is not applicable (e.g., in-channel, urban areas, etc.), a default roughness value is specified. In the Jarvela (2004) approach, the friction factor *f* is calculated as

$$f = 4C_{dX}\,\mathrm{LAI}\left(\frac{U}{U_X}\right)^X \frac{h}{H} \qquad 1$$

where C_{dX} is a species-specific drag coefficient, LAI is the leaf-area-index, X is a species-specific exponent, U is the flow velocity, and U_x is a reference velocity. The ratio of h (water depth) over H (plant height) is a scaling factor to account for partial submergence ($h<H$). The parameters C_{dX}, LAI, X, U_x, and H are measured in the field and are defined spatially in the ArcGIS input shapefile. The variable flow velocity and water depth are obtained from the coupled hydraulic solver, where U is calculated as the resultant of the horizontal velocity components at each grid cell. Thus the friction factor is a function of spatial variation in the plant parameters and spatial and temporal variation in the hydraulic variables. In practice, the Manning's n is used by the hydraulic solver and is computed from the friction factor as

$$n = \frac{R^{1/6}}{\sqrt{8g/f}} \qquad 2$$

where R is the hydraulic radius and g is the acceleration of gravity.

Roughness can alternatively be calculated using the Baptist (2007) approach according to

$$C_r = \sqrt{\frac{1}{(1/C_b^2) + (C_d m D H/2g)}} + \frac{\sqrt{g}}{\kappa} \ln\left(\frac{h}{H}\right) \qquad 3$$

where C_b is the Chezy bed coefficient, C_d is the drag coefficient, m is plant density, D is stem diameter, H is plant height, $\kappa = 0.41$ is the von Karman constant, and h is the flow depth. Thus the composite resistance coefficient C_r includes the effects of bed resistance, form drag of flow through the vegetation, and the boundary layer formed above the vegetation. For emergent vegetation, the logarithmic term in (3) is dropped since the resistance is only a function of the bed roughness and vegetative drag. For dense vegetation, the contribution of the bed roughness term may be considered insignificant compared to the contribution of the vegetative drag term. The parameters C_b, C_d, m, D, and H are measured in the field and defined spatially in the ArcGIS input shapefile. The resistance in (3) is converted to Manning's n as

$$n = \frac{1}{C_r} R^{1/6} \qquad 4$$

In (1)-(4), the water depth h and hydraulic radius R are treated equivalently as either (A) the water depth at each grid cell or (B) the average water depth over the wetted cells within each polygon defined by the shapefile.

Vegetation Lifecycle Module

The vegetation lifecycle module predicts spatially-distributed seed dispersal, establishment, growth, and removal in response to dynamic hydraulic conditions. The algorithms are based largely on a one-dimensional vegetation, hydraulics, and sediment transport simulation tool (SRH-1DV) in continuing development by Reclamation (Fotherby, 2013). Thus, the development of the vegetation lifecycle module described herein primarily represents a porting of algorithms from a one-dimensional to two-dimensional framework. The spatial distribution is delineated by polygons in an ArcGIS shapefile and species-specific parameters are provided in a text file. Any number of species can be simulated provided one or more differentiating characteristics for each species can be quantified through the input parameter file. The vegetation lifecycle evolves temporally with the solution to the hydraulic variables; a hydrograph and rating curve specify the dynamic input and output boundary conditions (Lai, 2010). An initial establishment of vegetation can be specified for each polygon in the shapefile.

In the SRH-2DV model, plants establish at grid cells based on seed dispersal and suitability criteria. During the species-specific germination window, seeds are dispersed to every cell in the computational grid. Density ranging from 0 to 1 can be specified within each polygon in the input shapefile, and is treated as a probability of occurrence within individual grid cells. Each plant is allowed to grow based on age-specific rates given as input. The model tracks root depth & width, canopy width, and plant height. Root depth is limited by ground water elevation, which is assumed to be equal to the water elevation of the nearest wetted cell. Processes in the model that may kill a plant include age, scour, desiccation, and inundation. Species competition is not treated explicitly; however, dynamic conditions may favor the growth of one species over another. The effect of desiccation and inundation are a function of the age of the plant and cumulative duration of drying or wetting. The scour threshold for each species is dependent on the age of the plant, where increasing time since establishment is generally associated with higher resistance to removal.

Existing Model

The vegetation modules were tested by simulating a reach of the San Joaquin River in California's Central Valley. A computational mesh with boundary conditions was available for the reach from previous hydraulic modeling in support of the San Joaquin River Restoration Project (Dombroski, Greimann, & Gordon, 2012). The existing model was calibrated by comparing simulated water surface elevation to measured water surface elevation at a similar discharge. The Manning's *n* was then manually adjusted in the channel and floodplain areas in order to bring the simulated water surface elevation in better agreement with the measurements. Manually adjusting the Manning's *n* in order to effect the water surface elevation is generally successful in reproducing the gross effect of bed and

form roughness; however, the approach includes no explicit treatment of roughness due to vegetation, which limits the capability of the model in predicting vegetative effects.

Empirical Data and Field Work

Predicting vegetation-dependent hydraulic roughness and modeling vegetation lifecycle is dependent on empirical parameters that can only be determined through laboratory experiments or field studies. Thus, development and testing of the SRH-2DV vegetation modules was dependent on data reconnaissance in support of the modeled physical processes. A vegetation mapping study was performed that provided the basis for the input polygon shapefile containing spatial distribution information (Moise & Hendrickson, 2002) that was used in the hydraulic roughness module and vegetation lifecycle module. The species-dependent germination, growth, and stress parameters used in the lifecycle module are taken from prior work with the one-dimensional SRH-1DV vegetation module, and are documented elsewhere (Fotherby, 2013). A research group at the University of New Mexico performed a field study of vegetation along the San Joaquin River and initial testing of the SRH-2DV hydraulic roughness module (Gillihan, 2013). During the field campaign, measurements of vegetation height, stem diameter, density, and LAI were made in six 1000 ft^2 blocks along the river reach. In computing roughness according to the Jarvela (2004) approach, the parameters C_{dX}, X, U_x were taken from the literature (Aberle & Jarvela, 2013) and assumed uniform for all species. In computing roughness according to the Baptist (2007) approach, the parameter $C_D = 1.0$ was assumed for all species. The coefficient C_b was set to a value of 80 which is physically equivalent to assuming that the bed roughness is insignificant compared to the vegetation-induced roughness. Table 1 and Table 2 contain a source summary of the parameter values and variables used in the Jarvela (2004) and Baptist (2007) approaches, respectively. Values listed as plant-specific are measured in the field for each classified vegetation type and values listed as variable are iteratively computed by the SRH-2D hydraulic solver. In Table 1, the parameters X and C_{dX} are listed as area-specific because they are assumed uncertain and are adjusted spatially during the calibration process.

Parameter	Value	Source
C_{dX}	Area-Specific	Aberle & Jarvela, 2013
X	Area-Specific	Aberle & Jarvela, 2013
U_x	0.328 ft/s	Aberle & Jarvela, 2013
LAI	Plant-Specific	Gillihan, 2013
H	Plant-Specific	Gillihan, 2013
U	Variable	SRH-2D Solver
h	Variable	SRH-2D Solver

Table 1. Identification of parameters and variables used in the Jarvela (2004) approach for computing hydraulic roughness. The approach was tested using two different values of the exponent *X* in Equation Error! Reference source not found.**. Values listed as plant-specific are measured in the field for each classified vegetation type and values listed as variable are iteratively computed by the SRH-2D hydraulic solver.**

Parameter	Value	Source
C_D	1.0	Baptist et al., 2007
C_b	80	Gillihan, 2013
m	Plant-Specific	Gillihan, 2013
D	Plant-Specific	Gillihan, 2013
H	Plant-Specific	Gillihan, 2013
h	Variable	SRH-2D Solver

Table 2. Identification of parameters and variables used in the Baptist (2007) approach for computing hydraulic roughness. Values listed as plant-specific are measured in the field for each classified vegetation type and values listed as variable are iteratively computed by the SRH-2D hydraulic solver.

Results

Hydraulic Roughness

The capability of the hydraulic roughness module in estimating roughness due to vegetation was evaluated by comparing computed Manning's *n* to manually calibrated Manning's *n* and by comparing computed water surface elevation to measured water surface elevation at a similar discharge. Also available for comparison is simulated water surface elevation from the manually calibrated model. Figure 2-Figure 4 show comparisons of water surface elevation results from simulated discharges of Q = 2500-7500 cfs using the Baptist (2007) approach and Jarvela (2004) approach for calculating hydraulic roughness due to vegetation. Also shown is water surface elevation from a simulation using manually calibrated roughness and field measurements of water surface elevation for a similar discharge. The results indicate that the Jarvela (2004) approach, although resulting in under predicted water surface elevation, performs better than the Baptist (2007) approach, and compares favorably with the performance of the manually calibrated model for large extents of the model reach.

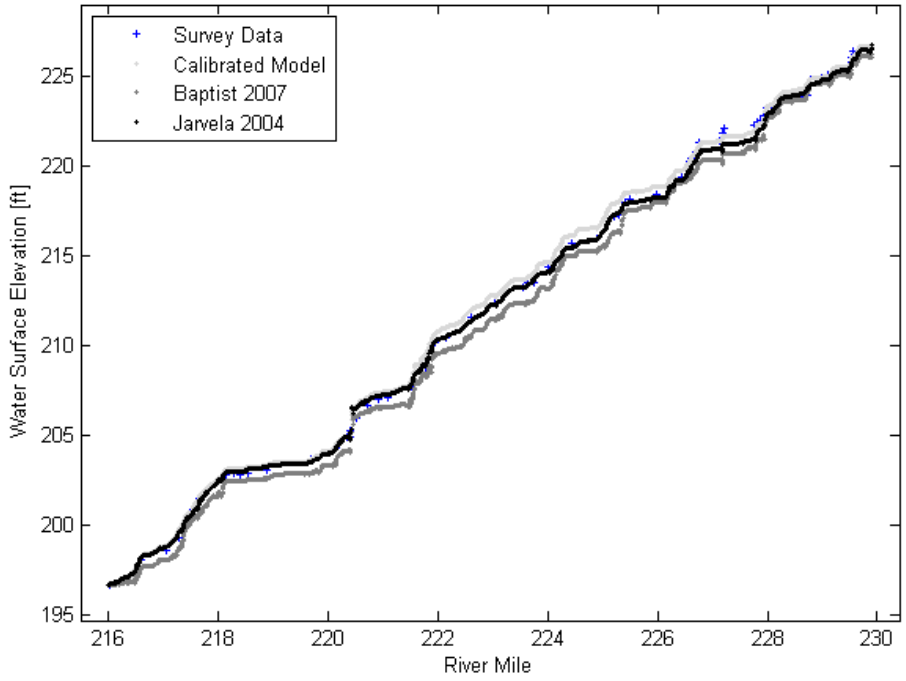

Figure 1. Simulated water surface elevation (ft) as a function of river mile (mi) for Q = 1100 cfs in a reach of the San Joaquin River. Shown for comparison are measured water surface elevation (blue), manually calibrated simulation results (light grey), simulation results using the Baptist (2007) approach (grey), and simulation results using the Jarvela (2004) approach (black). The figure demonstrates that the Jarvela (2004) approach performs better than the Baptist (2007) approach, and compares favorably with the performance of the manually calibrated model.

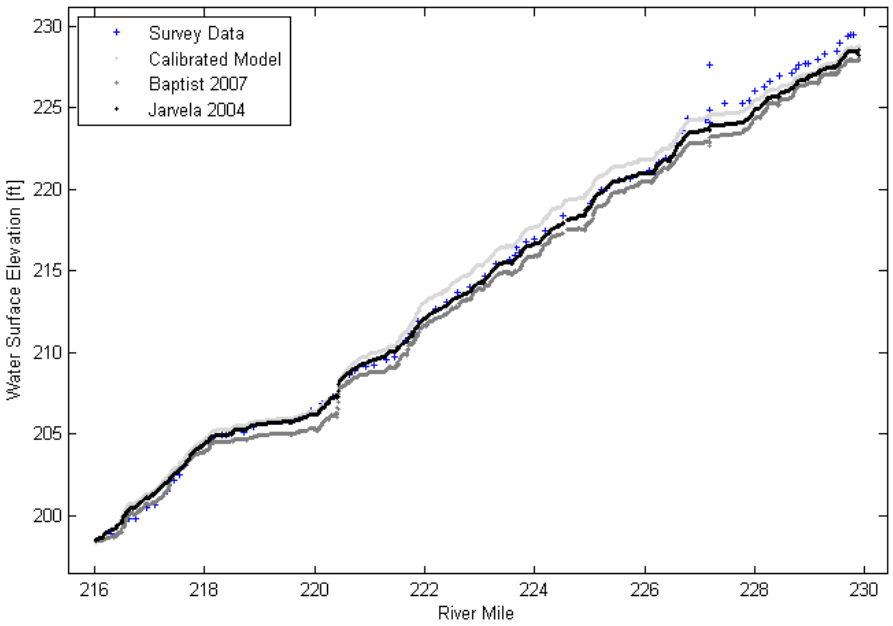

Figure 2. Simulated water surface elevation (ft) as a function of river mile (mi) for Q = 2500 cfs in a reach of the San Joaquin River. Shown for comparison are measured water surface elevation (blue), manually calibrated simulation results (light grey), simulation results using the Baptist (2007) approach (grey), and simulation results using the Jarvela (2004) approach (black). The figure demonstrates that the Jarvela (2004) approach performs better than the Baptist (2007) approach, and compares favorably with the performance of the manually calibrated model.

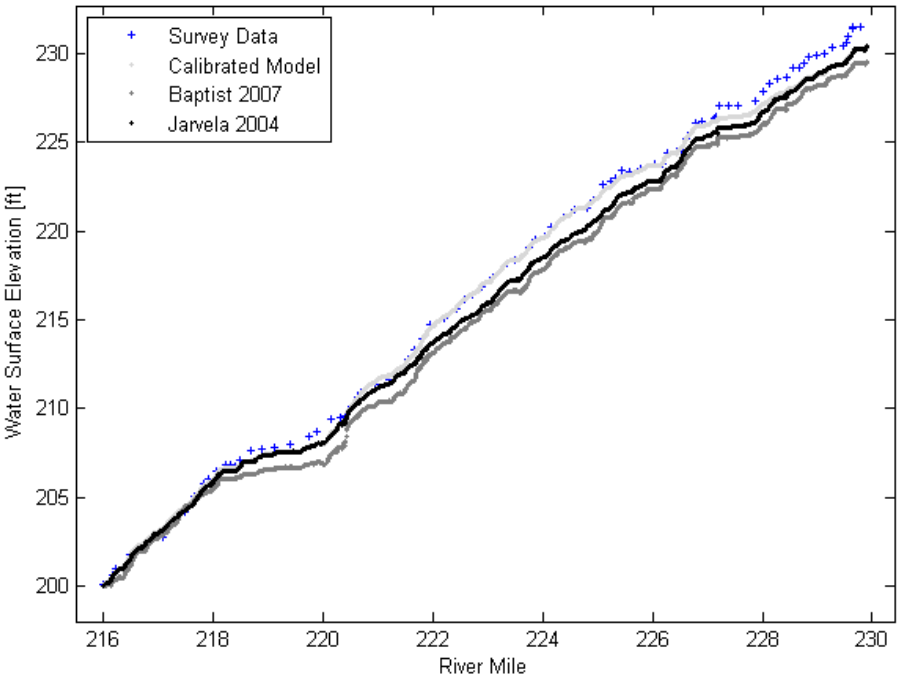

Figure 3. Simulated water surface elevation (ft) as a function of river mile (mi) for Q = 4000 cfs in a reach of the San Joaquin River. Shown for comparison are measured water surface elevation (blue), manually calibrated simulation results (light grey), simulation results using the Baptist (2007) approach (grey), and simulation results using the Jarvela (2004) approach (black). The figure demonstrates that the Jarvela (2004) approach performs better than the Baptist (2007) approach, although falls short of the performance of the manually calibrated model.

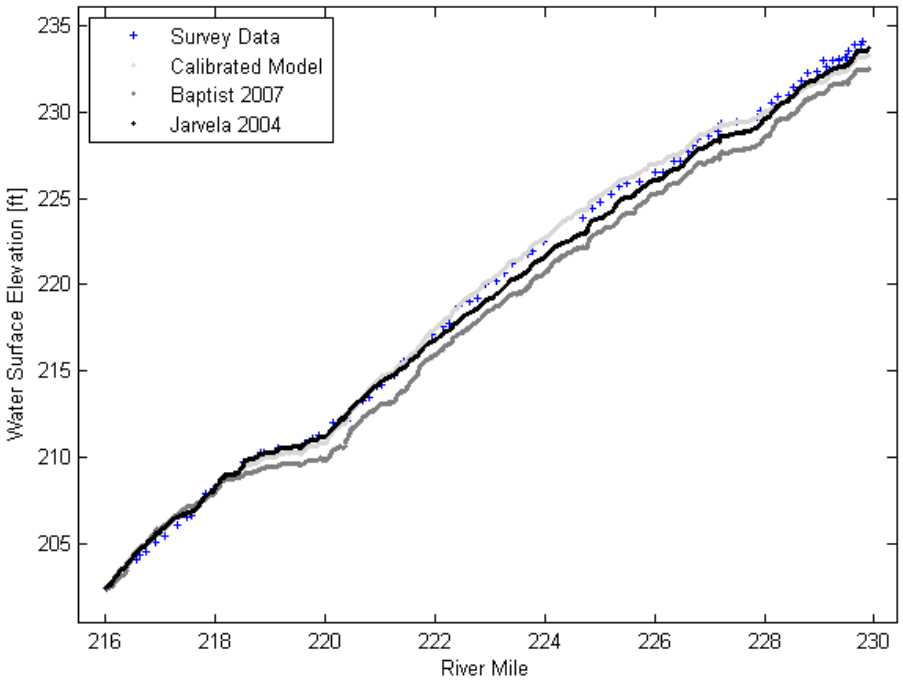

Figure 4. Simulated water surface elevation (ft) as a function of river mile (mi) for Q = 7500 cfs in a reach of the San Joaquin River. Shown for comparison are measured water surface elevation (blue), manually calibrated simulation results (light grey), simulation results using the Baptist (2007) approach (grey), and simulation results using the Jarvela (2004) approach (black). The figure demonstrates that the Jarvela (2004) approach performs better than the Baptist (2007) approach, although falls short of the performance of the manually calibrated model.

The simulated water surface elevation is in part determined by the distribution of Manning's *n* values computed by the model for each vegetation type. Compiled in Figure 5 through Figure 10 are distributions of Manning's *n* values for some well-represented vegetation types in the modeled reach of the San Joaquin River. The distributions are compiled from the Manning's *n* value at each cell in the computational mesh as designated by the vegetation type polygons. The distributions shown in each figure include (A) the calculated values for wetted cells using the Jarvela (2004) approach, (B) the polygon values including those calculated in wet cells and the default value of n=0.035 in dry cells, and (C) the values taken from the manually calibrated model. Also shown in each plot are the mean (solid line) and standard deviation from the mean (dashed line) of the calculated Manning's *n* values for wetted cells. The distribution of calculated Manning's *n* values (blue) in each plot is representative of cells that are directly coupled to the hydraulics through (**Error! Reference source not found.**). For Mixed Riparian (Figure 5), Willow Riparian (Figure 6), and Cottonwood Riparian (Figure 7) vegetation types, the compilation of Manning's *n* values are approximately normally distributed around the mean value. Manning's *n* values calculated for the Willow Scrub (Figure 8) vegetation type do not appear to be normally distributed, possibly due to species-specific parameters that are causing the calculated roughness values to be biased low. The cumulative count of a distribution of Manning's *n* values provides an indication of the relative influence

a given vegetation type has in the hydraulic computations the model is performing. The gross effects of vegetative roughness in the hydraulic model will be driven by vegetation types that are largely inundated for the flow simulated. In the model reach of the San Joaquin River, many cells within the computational mesh are classified as Agricultural Field (Figure 10). The count of calculated Manning's values is far less, however, indicating that the portion of inundated agricultural field (and therefore the effect of agricultural vegetation on the hydraulics within the reach) is small.

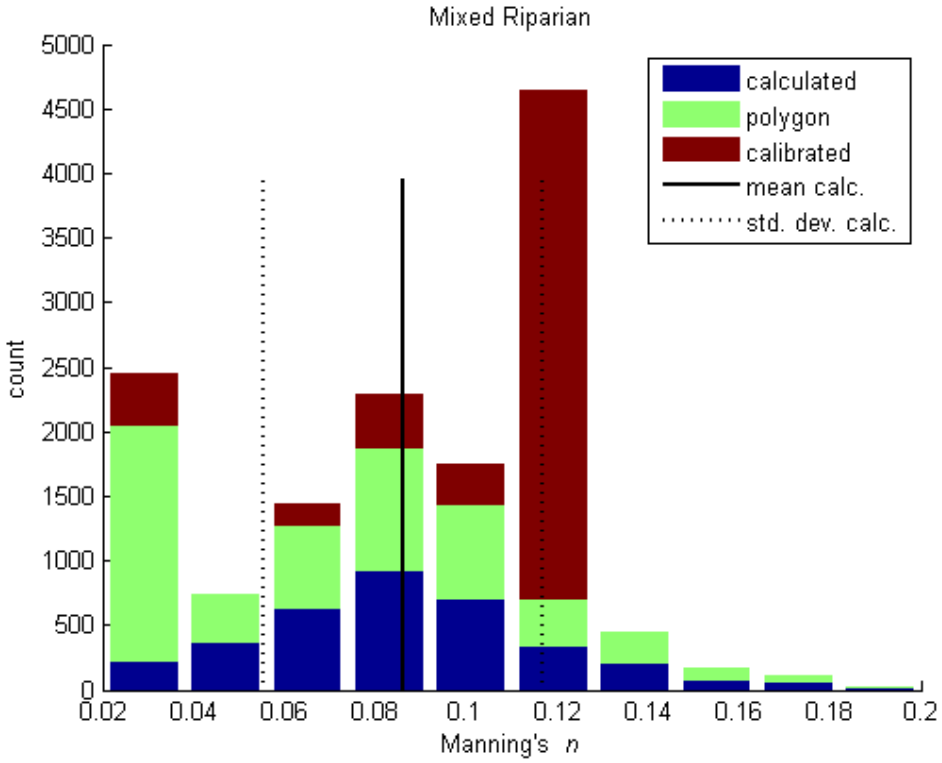

Figure 5. Distribution of Manning's *n* values for Mixed Riparian vegetation in the computational mesh of the modeled reach of the San Joaquin River. Shown in the figure are the calculated values for wetted cells using the Jarvela (2004) approach (blue), the polygon values including those calculated in wet cells and default values in dry cells (green), and the values taken from the manually calibrated model (red). Also shown are the mean (solid line) and standard deviation from the mean (dashed line) of the calculated Manning's *n* values for wetted cells.

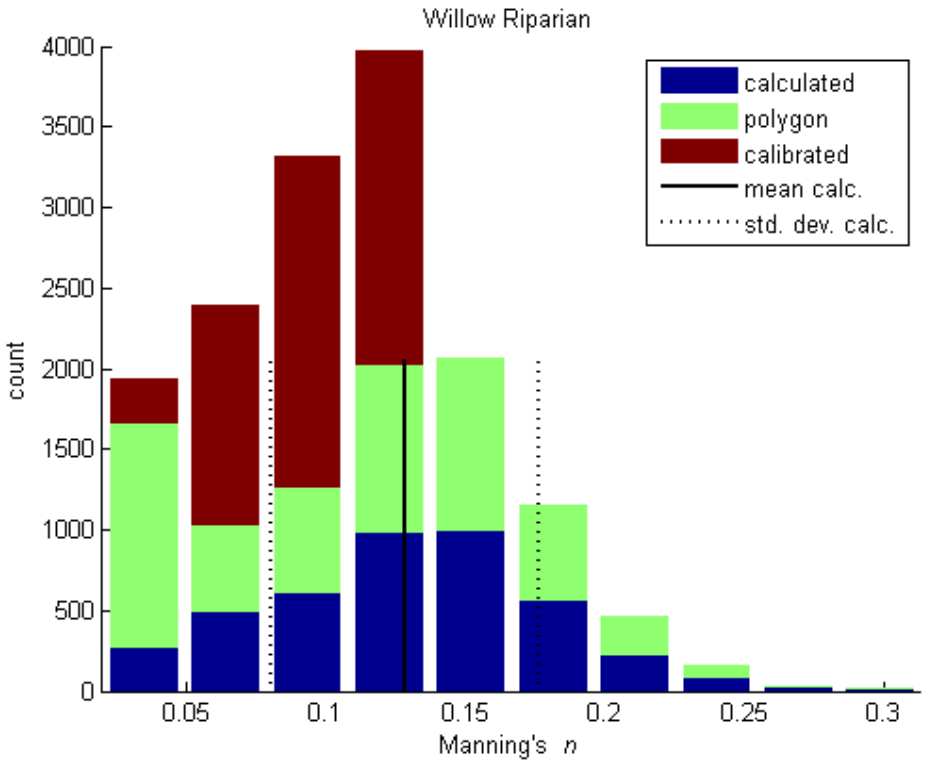

Figure 6. Distribution of Manning's *n* values for Willow Riparian vegetation in the computational mesh of the modeled reach of the San Joaquin River. Shown in the figure are the calculated values for wetted cells using the Jarvela (2004) approach (blue), the polygon values including those calculated in wet cells and default values in dry cells (green), and the values taken from the manually calibrated model (red). Also shown are the mean (solid line) and standard deviation from the mean (dashed line) of the calculated Manning's *n* values for wetted cells.

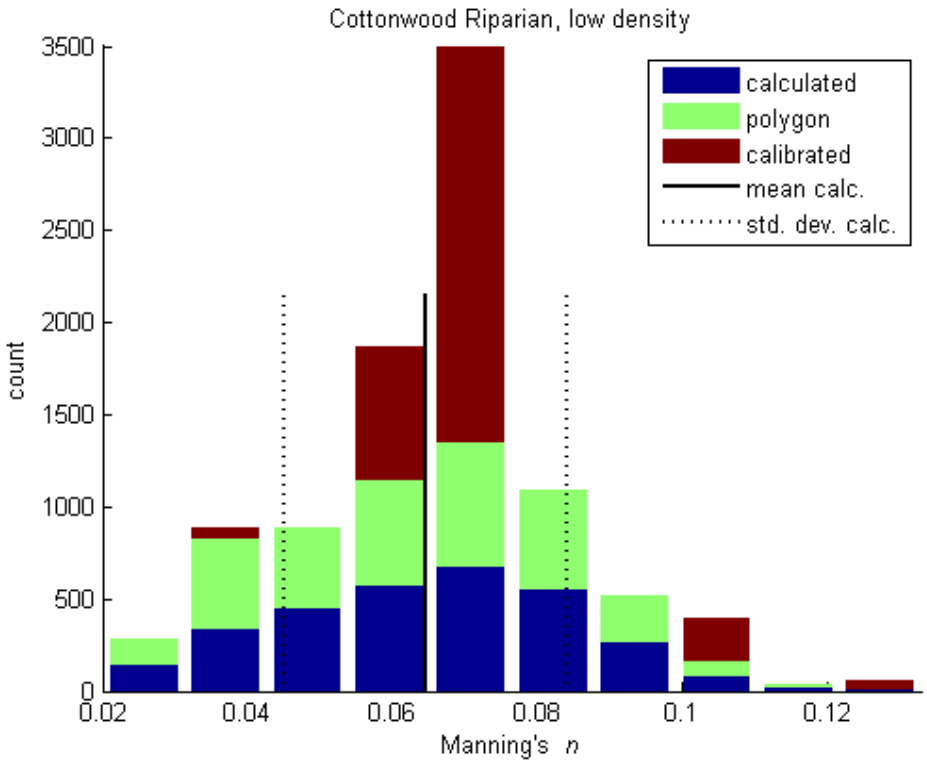

Figure 7. Distribution of Manning's *n* values for Cottonwood Riparian vegetation in the computational mesh of the modeled reach of the San Joaquin River. Shown in the figure are the calculated values for wetted cells using the Jarvela (2004) approach (blue), the polygon values including those calculated in wet cells and default values in dry cells (green), and the values taken from the manually calibrated model (red). Also shown are the mean (solid line) and standard deviation from the mean (dashed line) of the calculated Manning's *n* values for wetted cells.

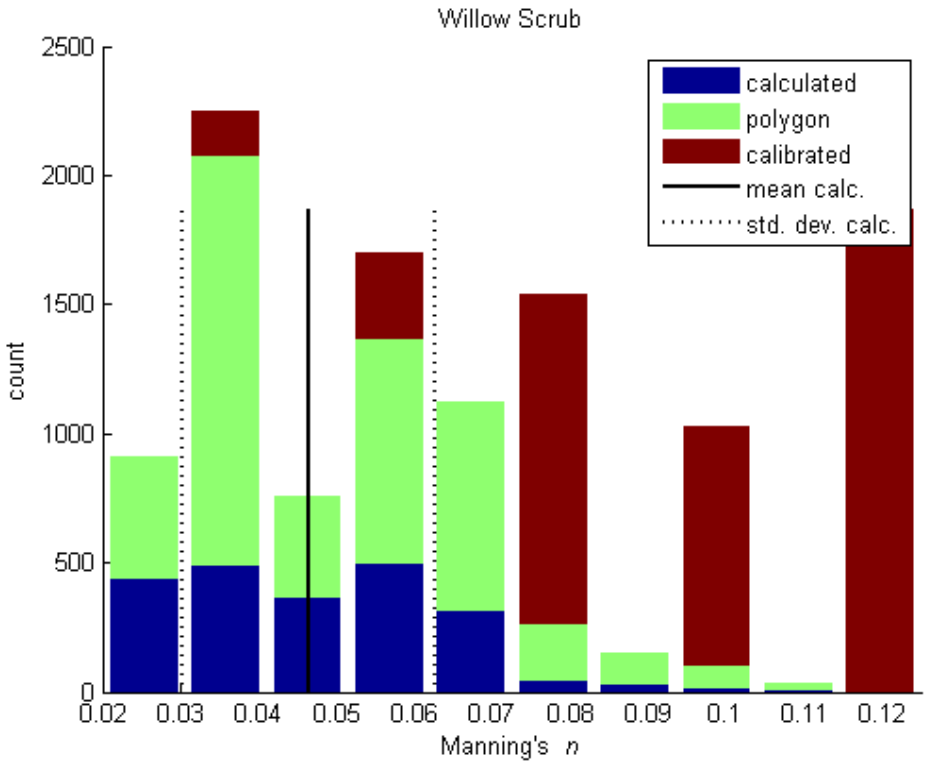

Figure 8. Distribution of Manning's *n* values for Willow Scrub vegetation in the computational mesh of the modeled reach of the San Joaquin River. Shown in the figure are the calculated values for wetted cells using the Jarvela (2004) approach (blue), the polygon values including those calculated in wet cells and default values in dry cells (green), and the values taken from the manually calibrated model (red). Also shown are the mean (solid line) and standard deviation from the mean (dashed line) of the calculated Manning's *n* values for wetted cells.

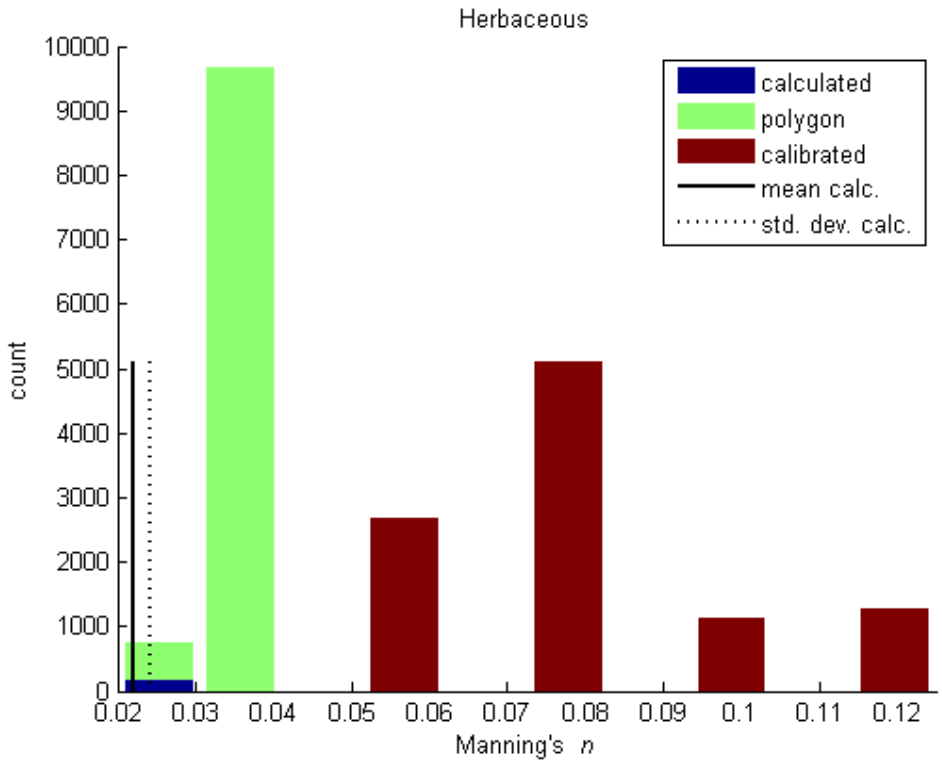

Figure 9. Distribution of Manning's *n* values for Herbaceous vegetation in the computational mesh of the modeled reach of the San Joaquin River. Shown in the figure are the calculated values for wetted cells using the Jarvela (2004) approach (blue), the polygon values including those calculated in wet cells and default values in dry cells (green), and the values taken from the manually calibrated model (red). Also shown are the mean (solid line) and standard deviation from the mean (dashed line) of the calculated Manning's *n* values for wetted cells.

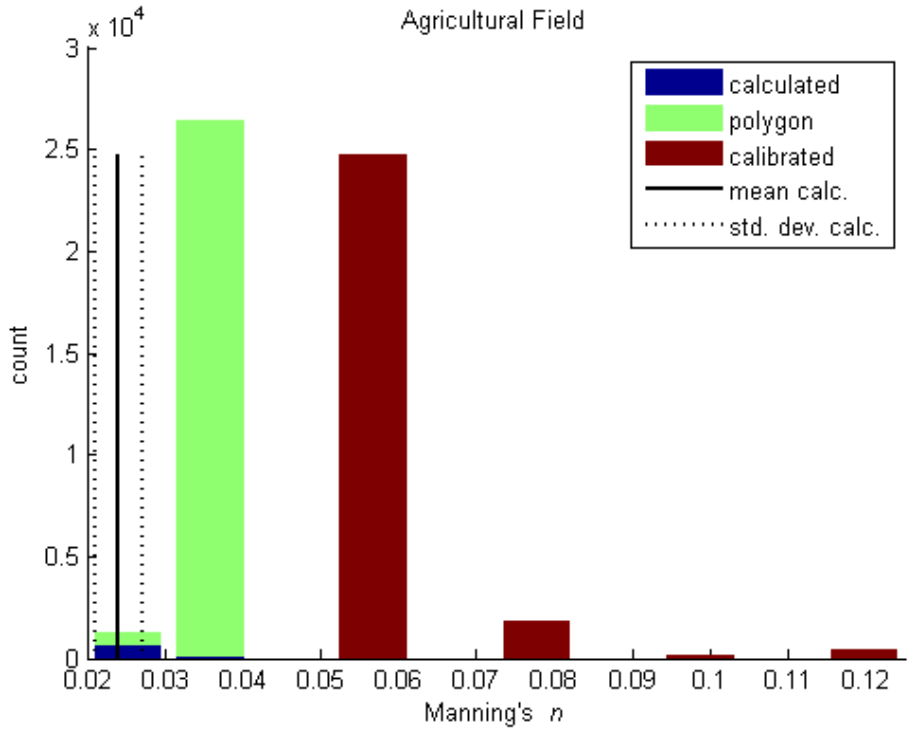

Figure 10. Distribution of Manning's *n* values for Agricultural Field vegetation in the computational mesh of the modeled reach of the San Joaquin River. Shown in the figure are the calculated values for wetted cells using the Jarvela (2004) approach (blue), the polygon values including those calculated in wet cells and default values in dry cells (green), and the values taken from the manually calibrated model (red). Also shown are the mean (solid line) and standard deviation from the mean (dashed line) of the calculated Manning's *n* values for wetted cells.

The comparisons in Figure 1 - Figure 4 show that water surface elevation is underestimated in approximately the upper 2/3 of the model reach using the Jarvela (2004) approach for calculating roughness. This suggests that preferentially increasing the roughness in the upper portion of the model reach may produce simulated hydraulics that better match observed conditions. The mean calculated roughness values for the mixed riparian (Figure 5) and willow scrub (Figure 8) vegetation types tend lower than the bulk of calibrated roughness values for the same types, which raises the question of whether the spatial distribution of mixed riparian and willow scrub vegetation types may be correlated to the underestimation of water surface elevation in the upper portion of the model reach. Upon inspection of the spatial distribution of mixed riparian and willow scrub vegetation types within the model reach (Figure 11), it is apparent that there is greater spatial coverage in the upper 2/3 of the reach. It was therefore hypothesized that tuning the parameters for the mixed riparian and willow scrub vegetation in order to increase calculated roughness for these types would result in simulated hydraulics that better match the observed conditions. The species-specific drag coefficient C_{dX} was increased from 0.43 to 0.75 for only the mixed riparian and willow scrub types and the model was run again using the Jarvela (2004) approach for calculating roughness.

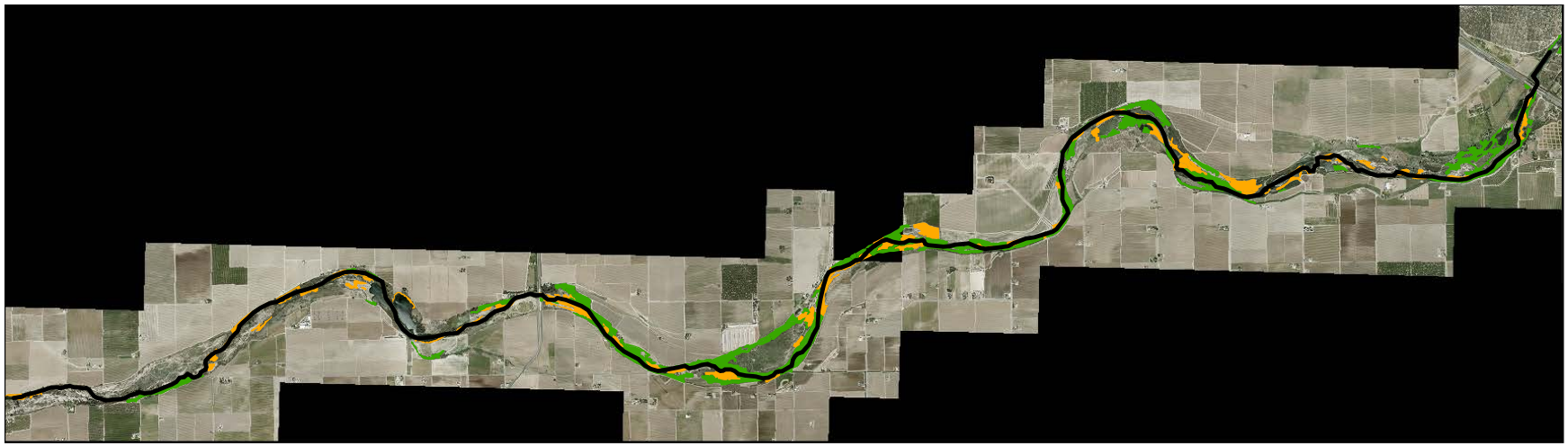

Figure 11. Aerial imagery of the model reach with overlay of mixed riparian (green) and willow scrub (orange) vegetation types. The channel centerline is delineated by the solid black line. Qualitatively, the mixed riparian and willow scrub vegetation types cover greater spatial extent in the upper 2/3 of the model reach than in the lower portion, which suggests that the corresponding vegetation type parameters may preferentially effect the simulated hydraulics in the upper portion of the reach.

A comparison of water surface elevation for variation in the parameter C_{dX} for a simulated discharge of Q = 7500 cfs is shown in Figure 12. The comparison demonstrates that increasing the species-specific drag coefficient C_{dX} for the mixed riparian and willow scrub vegetation positively affected the simulated hydraulics by preferentially increasing water surface elevation through regions of the modeled reach that were underestimated using a constant value C_{dX}. The distribution of resulting roughness values is shown in Figure 13; in comparison to Figure 5, variation in parameter C_{dX} resulted in a shift in the distribution of calculated roughness towards larger values. Another test of parameter sensitivity was conducted by varying the exponent X in (**Error! Reference source not found.**) for the mixed riparian and willow scrub vegetation types. Increasing the fractional exponent X has the effect of increasing roughness, however, with a less than linear sensitivity. For the trial simulation, X was increased from -0.57 to -0.35 for the mixed riparian and willow scrub vegetation types, however the effect on the simulated water surface elevation was small compared to the effect when varying the drag coefficient, C_{dX}. Comparison of water surface elevation at additional discharges and sensitivity analysis for varying input parameters is provided in Gillihan (2013).

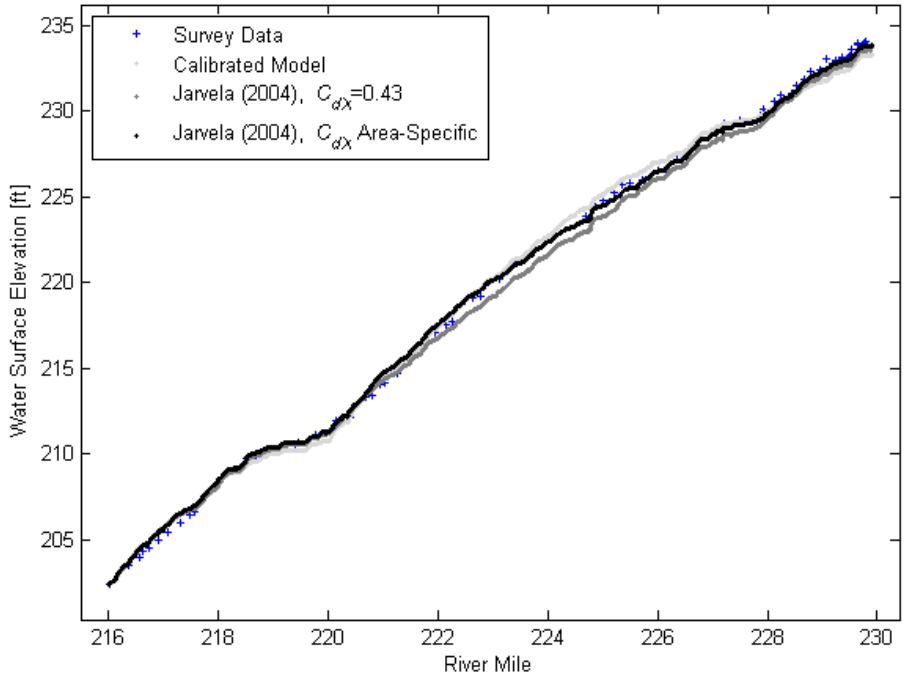

Figure 12. Simulated water surface elevation (ft) as a function of river mile for Q=7500 cfs in a reach of the San Joaquin River. Simulation results are shown for the Jarvela (2004) approach using constant C_{dX}=0.43 (grey) for all vegetation and C_{dX}=0.75 (black) for mixed riparian and willow scrub vegetation. Shown for comparison are measured water surface elevation (blue) and manually calibrated simulation results (light grey). The comparison demonstrates that increasing the species-specific drag coefficient C_{dX} for the mixed riparian and willow scrub vegetation positively affected the simulated hydraulics by preferentially increasing water surface elevation through regions of the modeled reach that were underestimated using a constant value C_{dX}.

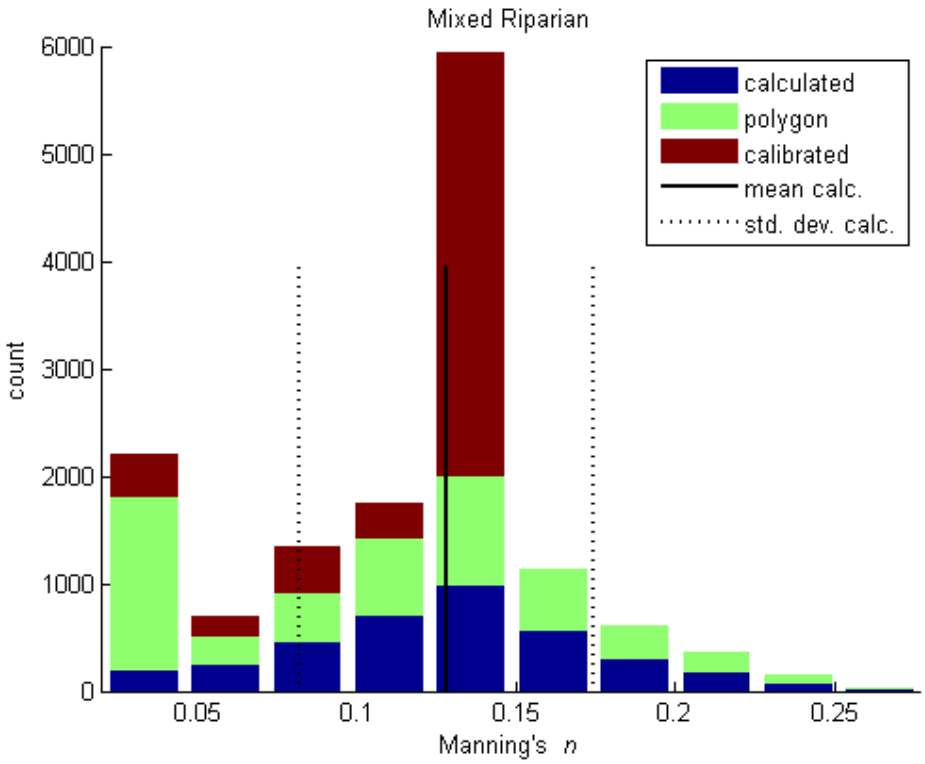

Figure 13. Distribution of Manning's *n* values for Mixed Riparian vegetation in the computational mesh of the modeled reach of the San Joaquin River. Shown in the figure are the calculated values for wetted cells using an area-specific parameter C_{dX} in the Jarvela (2004) approach (blue), the polygon values including those calculated in wet cells and default values in dry cells (green), and the values taken from the manually calibrated model (red). Also shown are the mean (solid line) and standard deviation from the mean (dashed line) of the calculated Manning's *n* values for wetted cells. In comparison to Figure 5, the variation in parameter C_{dX} resulted in a shift in the distribution of calculated roughness towards larger values.

Vegetation Lifecycle

The utility of the vegetation lifecycle module was demonstrated by performing a dynamic simulation of six vegetation species common to Western riparian zones (invasive and native): Arundo, Cottonwood, Goodings Black Willow, herbacious, Narrow Leaf Willow, and Red Sespania. Description of vegetation types and model input parameters are provided in Fotherby (2013). Differences in defining characteristics of vegetation species are specified in the input file through (A) germination constraints, (B) growth rate, (C) scour resistance, (D) inundation duration, (E) desiccation susceptibility, and (F) life expectancy. A hypothetical input hydrograph was generated to specify the temporal variation of flow through the hydraulic model (Figure 14).

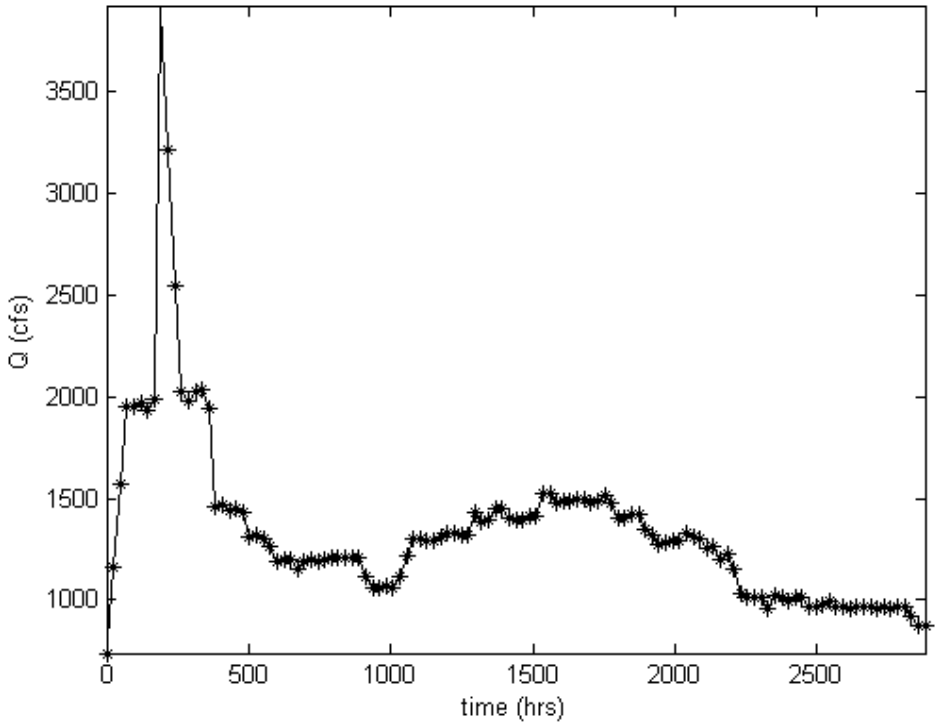

Figure 14. Input hydrograph specifying dynamic flow Q (cfs) as a function of time (hrs) for simulation of hydraulics and vegetation lifecycle.

The simulated establishment of Arundo, Cottonwood, Goodings Black Willow, herbaceous, Narrow Leaf Willow, and Red Sespania are shown in Figure 15-Figure 20, respectively, for a subsection of the modeled reach of the San Joaquin River. Also shown in the figures are designated no growth areas, simulated water depth, and background aerial imagery. The distribution and extent of vegetation in each image demonstrates that hydraulics and species-specific parameters impart species specificity to the predicted establishment. This provides a means for predicting inter-species differences in response to set conditions and intra-species differences in response to varying conditions.

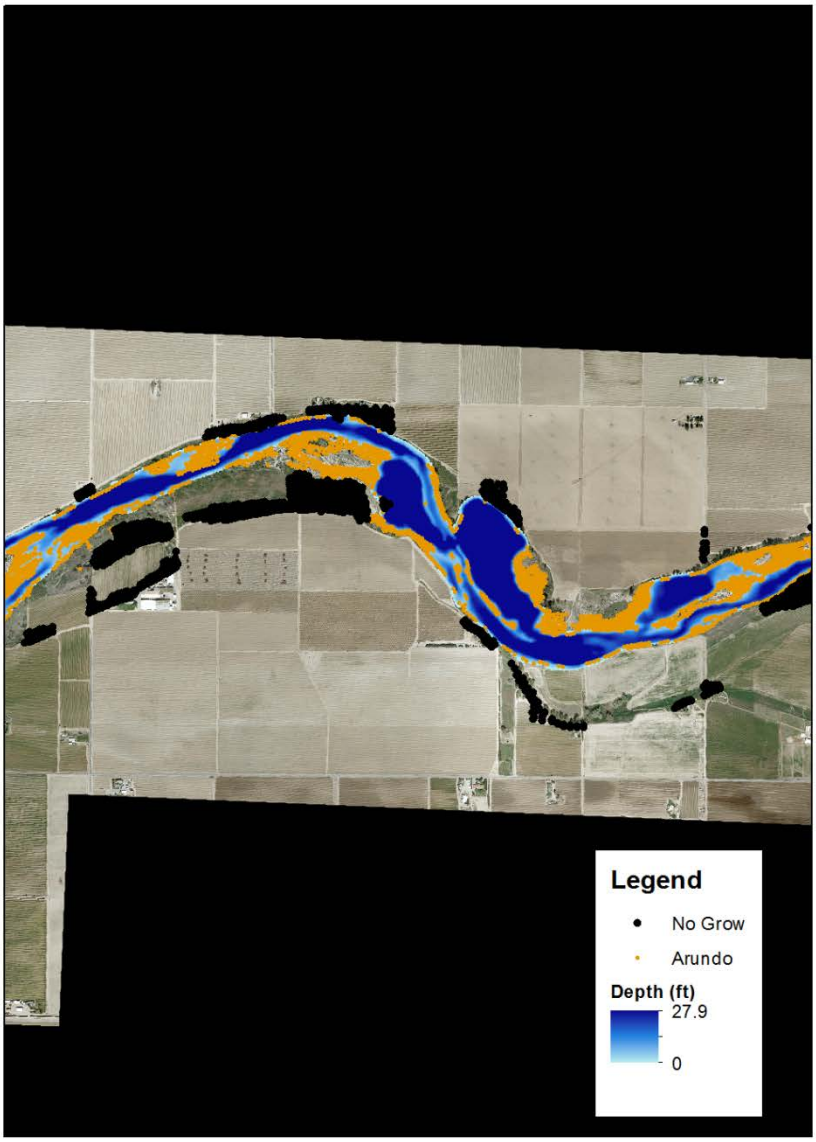

Figure 15. Simulated establishment of Arundo in subsection of San Joaquin River. Also shown in the figure are designated no growth areas, simulated water depth, and background aerial imagery.

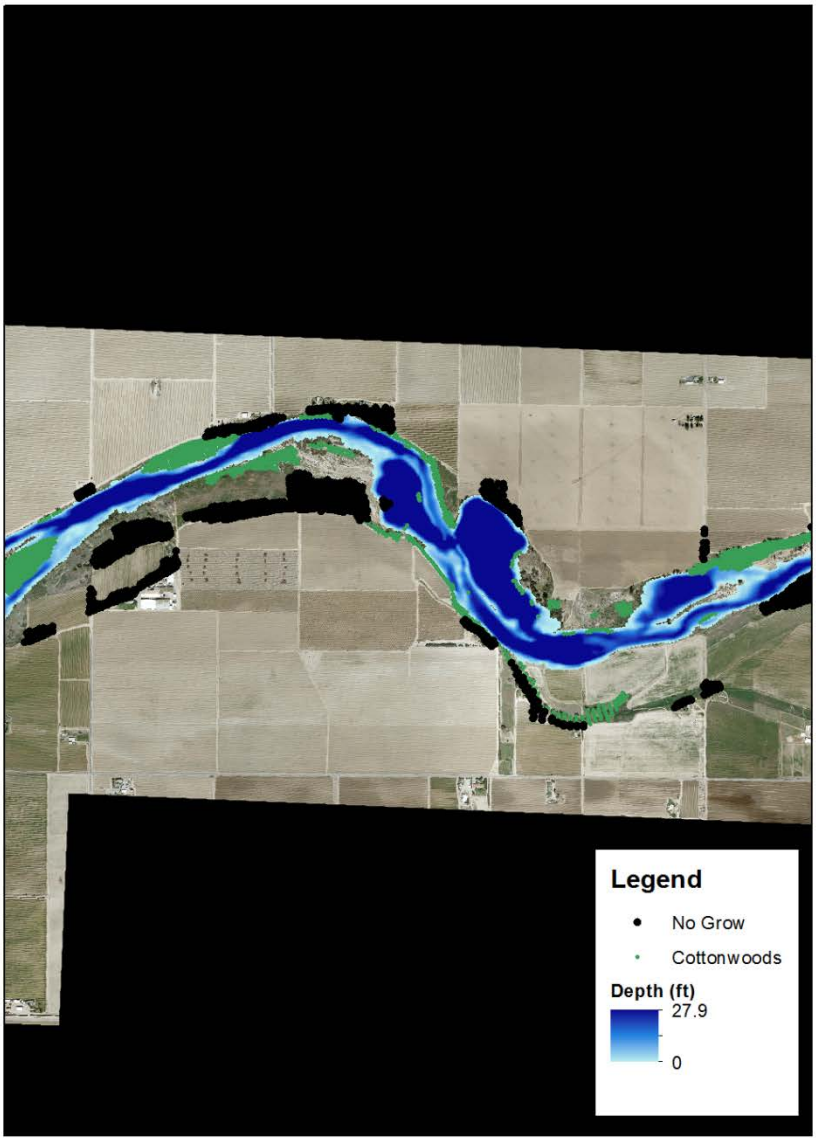

Figure 16. Simulated establishment of Cottonwood in subsection of San Joaquin River. Also shown in the figure are designated no growth areas, simulated water depth, and background aerial imagery.

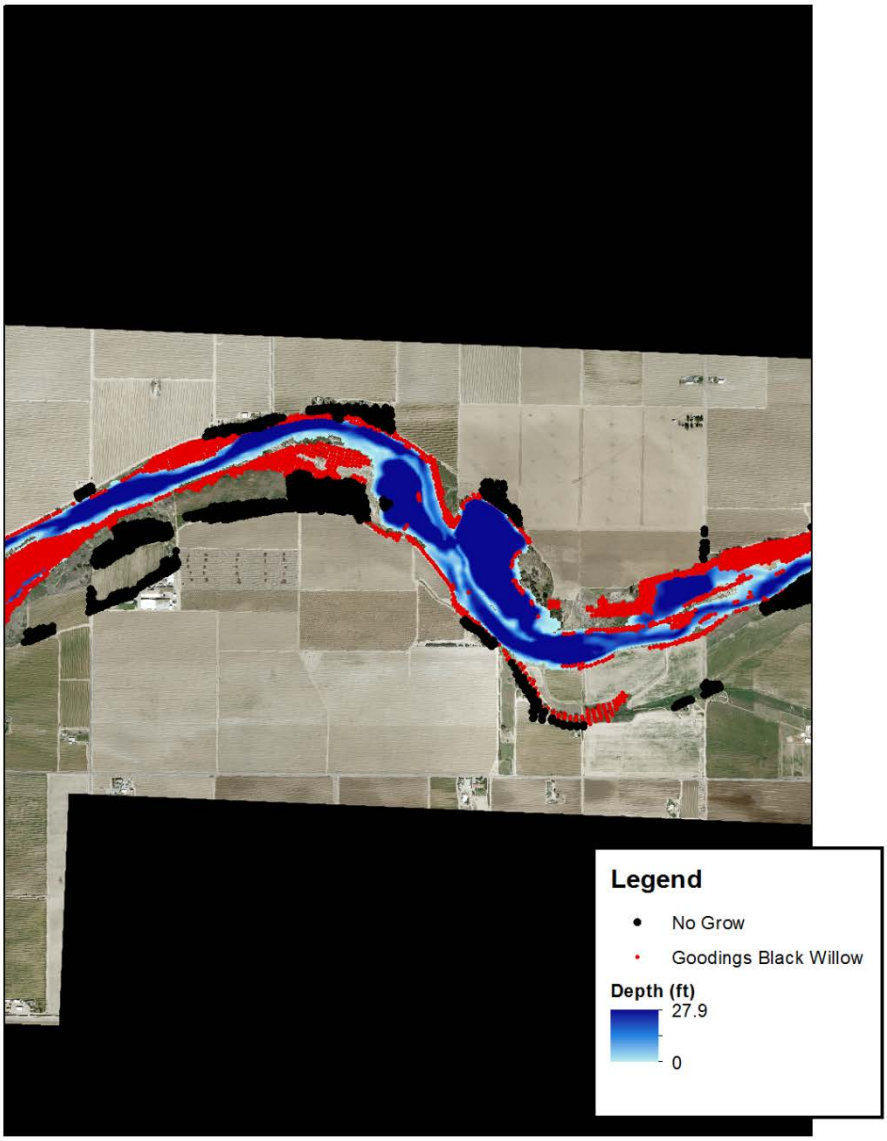

Figure 17. Simulated establishment of Goodings Black Willow in subsection of San Joaquin River. Also shown in the figure are designated no growth areas, simulated water depth, and background aerial imagery.

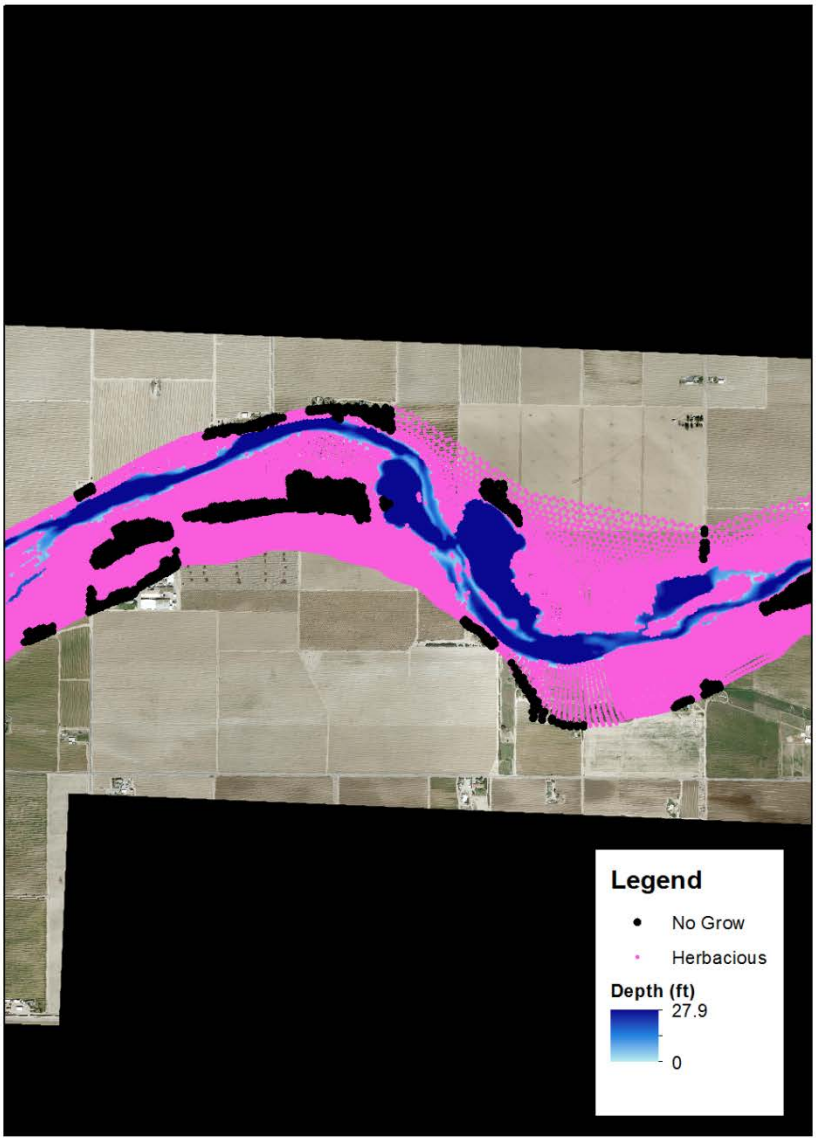

Figure 18. Simulated establishment of herbaceous vegetation in subsection of San Joaquin River. Also shown in the figure are designated no growth areas, simulated water depth, and background aerial imagery.

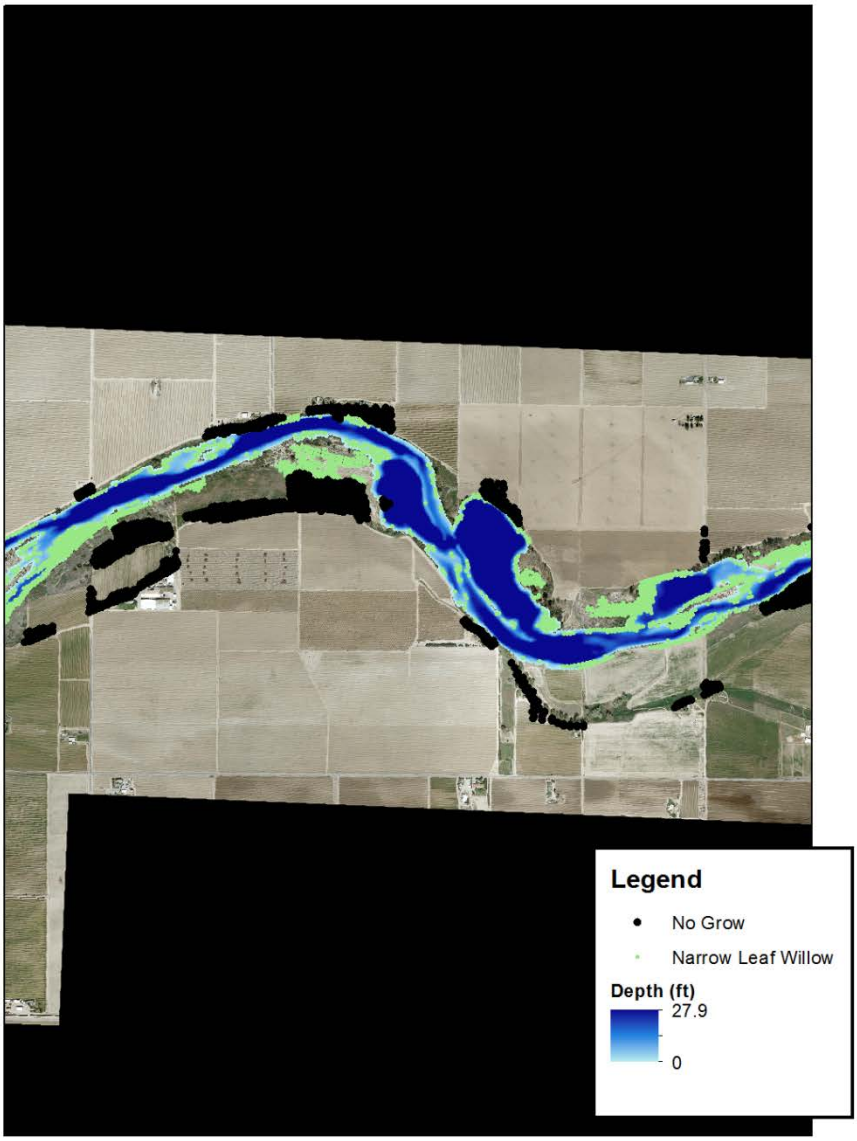

Figure 19. Simulated establishment of Narrow Leaf Willow in subsection of San Joaquin River. Also shown in the figure are designated no growth areas, simulated water depth, and background aerial imagery.

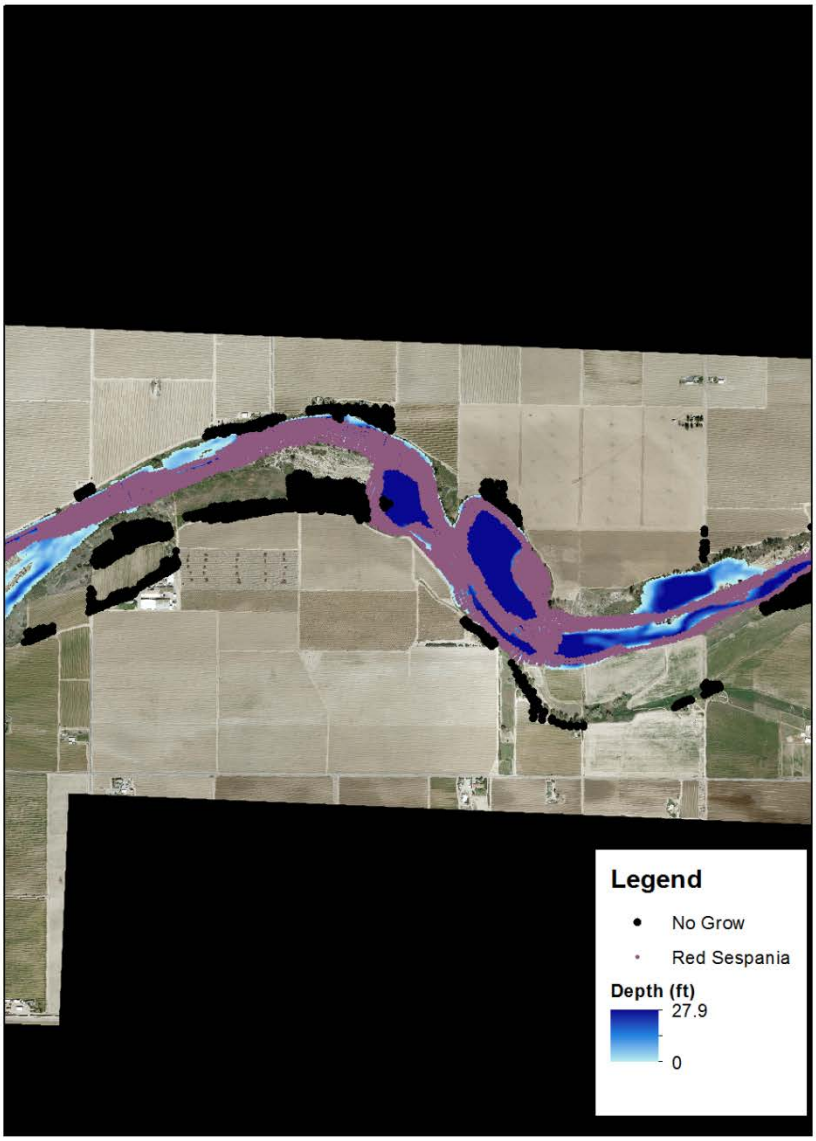

Figure 20. Simulated establishment of Red Sespania in subsection of San Joaquin River. Also shown in the figure are designated no growth areas, simulated water depth, and background aerial imagery.

Conclusions

The results demonstrate that the vegetation model for computing hydraulic roughness is generally successful in reproducing the effect of riparian vegetation on water surface elevation as compared to that of measurements and manually calibrated simulations. Distributions of calculated roughness values due to vegetation were generally consistent with values compiled in the literature (Hession & Curran, 2013). The Jarvela (2004) and Baptist (2007) approaches for computing roughness were both implemented in the model, although the Jarvela (2004) approach was more thoroughly evaluated through variation in equation parameters. The calibration procedure assumed variables computed by the hydraulic solver (U, h) and vegetation characteristics measured in the field (LAI, H) to be known quantities; the parameters C_{dX} and X were assumed uncertain and subject to variation. This procedure could be analogously applied to calibrate the Baptist (2007) approach; however, the input parameters (m, D) require a different set of field measurements. The leaf area index is generally a convenient physically-based metric for quantifying vegetal density and area (Jalonen, Jarvela, & Aberle, 2013), and can be estimated by in situ observation or remote sensing. Further, the Jarvela (2004) approach incorporates water depth and velocity information, both of which are directly computed by the hydraulic solver. Given the spatially-detailed information that a two-dimensional hydraulic model can provide, it would be desirable to map input vegetation parameters at similar scale and resolution (Abu-Aly, Pasternack, Wyrick, Barker, Massa, & Johnson, 2014), which would necessitate the use of remote sensing technologies. The distributions of calculated roughness values produced by the model (Figure 5-Figure 10) and the effect of varying the parameter C_{dX} (Figure 12-Figure 13) in (**Error! Reference source not found.**) indicate that predicting the effects of vegetation on hydraulics is dependent on quantifying complicated species-specific coupling between the vegetation characteristics and local hydraulics. Further exploration of input parameter values and species dependency, a topic of active research (Aberle & Jarvela, 2013), would be useful in gauging applicability and evaluating performance of the algorithms. Despite the uncertainties and challenges involved, the vegetation module for computing hydraulic roughness will be a useful tool for predicting the effects of projected vegetation changes and for use as a design tool in restoring riparian vegetation.

The vegetation lifecycle module is capable of simulating the distribution of seedling establishment, plant growth, and vegetation removal in response to dynamic hydraulic conditions. Results from the model indicate that the predictions are qualitatively reasonable, however further testing would be required in order to verify accuracy for specific applications. It is likely that further development of algorithms for modeling physical processes would be required on a case-by-case basis in order to increase the applicability of the module to a wide variety of natural systems. For example, significant

assumptions regarding species competition, seed dispersal, and ground water may not be satisfactory in some cases. However, the primary utility of the vegetation lifecycle module is in gauging the differential effects of variation in operation, as opposed to predicting absolute end conditions. For this reason, it is likely that capturing dominant physical processes that may be directly affected by operational changes is sufficient for quantitatively predicting the effect of variation in hydraulic conditions on riparian vegetation.

Continuing development efforts will be focused on integration of the independent hydraulic roughness and lifecycle modules into a coupled framework with feedback interactions. The algorithms within each of the modules are highly empirical and require specific parameters. The primary challenge associated with the task of module integration is in developing relationships between conceptually similar (yet quantitatively distinct) parameters and variables. This is not only a challenge from a coding perspective, but also from a biological perspective. For example, leaf area index (used to predict hydraulic roughness) and vegetation canopy size (tracked in the vegetation lifecycle) are clearly interrelated; however, further work will be required in order to deterministically relate one to the other within the constraints of the model framework. Some physical processes, such as vegetation density, will need to be more directly modeled in the lifecycle algorithms in order to be applicable within the hydraulic roughness calculations.

References

Aberle, J., & Jarvela, J. (2013). Flow Resistance of Emergent Rigid and Flexible Floodplain Vegetation. *Journal of Hydraulic Research, 51*(1), 33-45.

Abu-Aly, T. R., Pasternack, G. B., Wyrick, J. R., Barker, R., Massa, D., & Johnson, T. (2014). Effects of LiDAR-derived, spatially distributed vegetation roughness on two-dimensional hydraulics in a gravel-cobble river at flows of 0.2 to 20 times bankfull. *Geomorph.*(206), 468-482.

Baptist, M., Babovic, V., Rodriguez Uthurburu, J., Keijzer, M., Uittenbogaard, R., Mynett, A., et al. (2007). On Inducing Equations for Vegetation Resistance. *Journal of Hydraulic Research, 45*(4), 435-450.

Chow, V. (1959). *Open-Channel Hydraulics.* New York: McGraw-Hill Co.

Darby, S. E. (1999). Effect of Riparian Vegetation on Flow Resistance and Flood Potential. *Journal of Hydraulic Engineering*, 443-454.

Dombroski, D., Greimann, B. P., & Gordon, E. (2012). *Hydraulic Studies for Fish Habitat Analysis.* Denver: Bureau of Reclamation.

Fathi-Moghadam, M., & Kouwen, N. (1997). Non-Rigid, Non-Submerged, Vegetation Roughness in Flood Plains. *Journal of Hydraulic Engineering*, 51-57.

Fotherby, L. (2013). *Vegetation Modeling with SRH-1DV.* Denver: Bureau of Reclamation Technical Service Center.

Gillihan, T. (2013). *Dynamic Vegetation Roughness in the Riparian Zone.* Master Thesis, University of New Mexico, Department of Civil Engineering.

Groves, J., Williams, D., Caley, P., Norris, R., & Caitcheon, G. (2009). Modeling of Floating Seed Dispersal in a Fluvial Environment. *River Research and Applications, 25*(5), 582-592.

Hession, W. C., & Curran, J. C. (2013). The Impacts of Vegetation on Roughness in Fluvial Systems. In J. F. Schroder, D. R. Butler, & C. R. Hupp (Eds.), *Treatise on Geomorphology* (Vol. 12, pp. 75-93). San Diego, CA: Academic Press.

Hooke, J., Brookes, C., Duane, W., & Mant, J. (2005). A Simulation Model of Morphological, Vegetation and Sediment Changes in Ephemeral Streams. *Earth Surface Processes and Landforms, 30*(7), 845-866.

Jalonen, J., Jarvela, J., & Aberle, J. (2013). Leaf Area Index as Vegetation Density Measure for Hydraulic Analyses. *J. Hydr. Eng., 139*(5), 461-469.

Jarvela, J. (2004). Determination of Flow Resistance Caused by Non-Submerged Woody Vegetation. *International Journal of River Basin Management, 2*(1), 61-70.

Jarvela, J. (2005). Effect of Submerged Flexible Vegetation on Flow Structure and Resistance. *Journal of Hydrology*, 233-241.

Kouwen, N., & Fathi-Moghadam, M. (2000). Friction Factors for Coniferous Trees Along rivers. *Journal of Hydraulic Engineering*, 732-740.

Kouwen, N., & Li, R.-M. (1980, June). Biomechanics of Vegetative Channel Linings. *Journal of the Hydraulics Division, Proceedings of the ASCE, 106*(HY6), 1085-1103.

Lai, Y. G. (1997). An Unstructured Grid Method for a Pressure-Based Flow and Heat Transfer Solver. *Numerical Heat Transfer, Part B*, 267-281.

Lai, Y. G. (2000). Unstructured Grid Arbitrarily Shaped Element Method for Fluid Flow Simulation. *AIAA Journal, 38*(12), 2246-2252.

Lai, Y. G. (2010). Two-Dimensional Depth-Averaged Flow Modeling with an Unstructured Hybrid Mesh. *Journal of Hydraulic Engineering, 136*(1), 12-23.

Lytle, D., & Merritt, D. (2004). Hydrologic Regimes and Riparian Forests: A Structured Population Model for Cottonwood. *Ecology, 85*(9), 634-645.

Mahoney, J., & Rood, S. (1998). Streamflow Requirements for Cottonwood Seedling Recruitment: An Integrative Model. *Wetlands, 18*(4), 634-645.

Meier, C. (2008). *Cottonwood Establishment in a Gravel-Bed River*. Ph.D. Thesis, University of Montana.

Merritt, D., & Wohl, E. (2002). Processes Governing Hydrochory Along Rivers: Hydraulics, Hydrology, and Dispersal Phenoogy. *Ecological Applications*, 1071-1087.

Moise, G. H., & Hendrickson, B. (2002). *Riparian Vegetation of the San Joaquin River.* State of California Department of Water Resources.

Nepf, H. M. (2012). Hydrodynamics of Vegetated Channels. *Journal of Hydraulic Research*, 262-279.

Perona, P., Camporeale, C., Perucca, E., Savina, M., Molnar, P., Burlando , P., et al. (2009). Modeling River and Riparian Vegetation Interactions and Related Importance for Sustainable Ecosystem Management. *Aquatic Sciences: Research Across Boundaries, 71*(3), 266-278.

Rood, S., Braatne, J., & Hughes, F. (2003). Ecophysiology of Riparian Cottonwoods: Stream Flow Dependency, Water Relations and Restoration. *Tree Physiology, 23*(16), 1113.

Shafroth, P., Wilcox, A., Lytle, D., Hickey, J., Andersen, D., Beauchamp, V., et al. (2010). Ecosystem Effects of Environmental Flows: Modeling and Experimental Floods in a Dryland River. *Freshwater Biology, 55*(1), 68-85.

Thompson, G. T., & Roberson, J. A. (1976). A Theory of Flow Resistance for Vegetated Channels. *Transactions of the ASAE*, 288-293.